Colloids and Surfaces, 12 (1984) 213—225
Elsevier Science Publishers B.V., Amsterdam — Printed in The Netherlands

BEHAVIOUR OF A LYOTROPIC-SMECTIC LIQUID CRYSTAL BETWEEN MICA SURFACES
A STUDY OF THE FULLY HYDRATED EGG-LECITHIN

LISBETH TER-MINASSIAN-SARAGA and ERIC PEREZ

Physico-Chimie des Surfaces et des Membranes, Equipe de Recherche du CNRS associée à l'Université René Descartes, UER Biomédicale, 45 rue des Saints-Pères, 75270 Paris cedex 06, (France)

(Received 18 July 1983; accepted in final form 18 April 1984)

ABSTRACT

The behaviour of three egg-lecithin (EL)—water (W) mixtures, 60% (w/w):I, 50% (w/w):II and 30% (w/w):III, squeezed out or sucked in between two mica surfaces was investigated using an apparatus designed by J.N. Israelachvili. Mixture I is a lyotropic-smectic liquid crystal (LSLC), in contrast to II and III in which the LSLC is in equilibrium with a separated phase of excess water. The force F applied to the mica-sheet holders, the "separation" D between the mica surfaces and the average refractive index were measured for $1 < D < 200$ nm.

A stepwise-thinning process was mainly observed on compressing mixtures I and II from separation $30 < D < 60$ nm down to the minimum reproducible separation D_{min}, 9.0 ± 0.7 nm, which corresponded to the flattening of the mica surfaces. The steps ΔD were equal to multiples of $\lambda = 5.5 \pm 0.4$ nm for sample I and of $\lambda = 5.3 \pm 0.3$ nm for sample II.

The contact area of the flattened-mica sheets increased with the force F at separation D_{min}. Assuming that an effective elastic parameter can be defined for our composite system (mica sheet + glue), we interpret the F—contact-area dependence using the theory of Johnson et al. and deduce values of average normal pressures or stresses of the order of 10 mN m^{-2} on the flat mica—mica contact. At such pressures the values of λ and the repeat distance of the LSLC formed by EL + W and measured by X-ray diffraction are similar.

The refractive index n of I is independent of separation for $D_{min} < D < 50$ nm but its value increases when D decreases for II and III. It appears that excess water is selectively extruded when F increases and D decreases. We suggest that, at maximum stress and $D_{min} = 9$ nm, the two mica surfaces are separated by two poorly hydrated EL bilayers, while the EL polar groups in contact with the mica surface are almost completely dehydrated.

INTRODUCTION

Structural forces and average refractive indices were reported for one thermotropic-nematic liquid-crystal (TNLC) drop squeezed between two curved-mica sheets at various separations [1]. The (large) size of the drop allowed one to neglect the contribution of the meniscus capillary forces

0166-6622/84/$03.00

to the measured surface forces. Both force and refractive-index variations originated in the small, central thin-film region of the liquid-crystal drop. The effects were significant at (assumed plane parallel) mica—mica-surface separations smaller than 15 nm.

No results were shown for the thermotropic-smectic liquid crystal (TSLC). It was, however, reported that this layered structure displays elastic behaviour and a stepwise thinning of the mid-portion of the drop after a large pushing force (on the mica sheets) is built up. These forces decay for the four to six layers closest to the mica surfaces, and they remain significant up to mica—mica separations of $\simeq 1\ \mu m$.

We report here the first results obtained [2] with a classical lyotropic-smectit liquid crystal (LSLC), namely the fully hydrated egg-lecithin (EL) [3]. This LSLC is more complex than the TSLC. It is a lamellar system formed by alternating aqueous W and EL bilayers at the composition EL/W = 60/40 (w/w).

At lower EL concentrations, the excess water forms a separate phase [4]. Therefore the pattern of squeezing out of LSLC, for example, may be different from that of TSLC and depends on the amount of water in the mixture.

Using an apparatus of the Israelachvili type [5], we have measured values of the forces F, separations D and the average refractive index n inbetween the two mica surfaces during either squeezing out or sucking in of three EL/W mixtures. Their compositions were, respectively, EL/W = 60/40 (w/w):I, 50/50 (w/w):II and 30/70 (w/w):III. The experiments were carried out with the sample in equilibrium with either saturated water vapour or liquid water.

Here, the experimental conditions are different from those of the studies described in Refs [1,3]. On compression, first excess water is extruded, and second, hydrated-lipid bilayers are expelled because our system is open to both EL and W. The thickness of these bilayers is expected to be pressure dependent, as shown in Ref. [3]. The technique developed by Israelachvili provides values for the applied forces. We have tried to deduce from the measured forces the values of the applied pressures.

MATERIALS AND METHODS

Materials

EL was obtained from Lipid Products (U.K.). The samples were prepared by incubating EL and the appropriate amount of tridistrilled water overnight at 0°C in an N_2 atmosphere. Except for sample I, which is a well-known LSLC [4], the samples included a separate phase of pure excess water in equilibrium with LSLC [4].

Methods

Apparatus

This has been described in Refs [1,5]. Its reliability was established by measuring the force versus distance with an aqueous 10^{-3} *M* NaCl solution and comparing the results with those reported in Ref. [5]. The results reported were obtained at room temperature: 20.5—24.5°C.

The reference (zero) separation between the flattened-mica surfaces was determined in air before each run. The radius of curvature R of the mica surfaces was measured in the presence of LSLC. The radius a of the mica—mica-contact area, assumed to be circular, was estimated using a 200 × magnifying device.

Description of a run (Fig. 1)

The runs were conducted on the same LSLC sample, first in the presence of saturated water vapour and then with the sample immersed in liquid water.

The cell was filled with water to a level where its surface was close to but below the force-measuring leaf spring. A large amount (about 0.1 ml) of LSLC, which had the appearance of a paste, was deposited with an

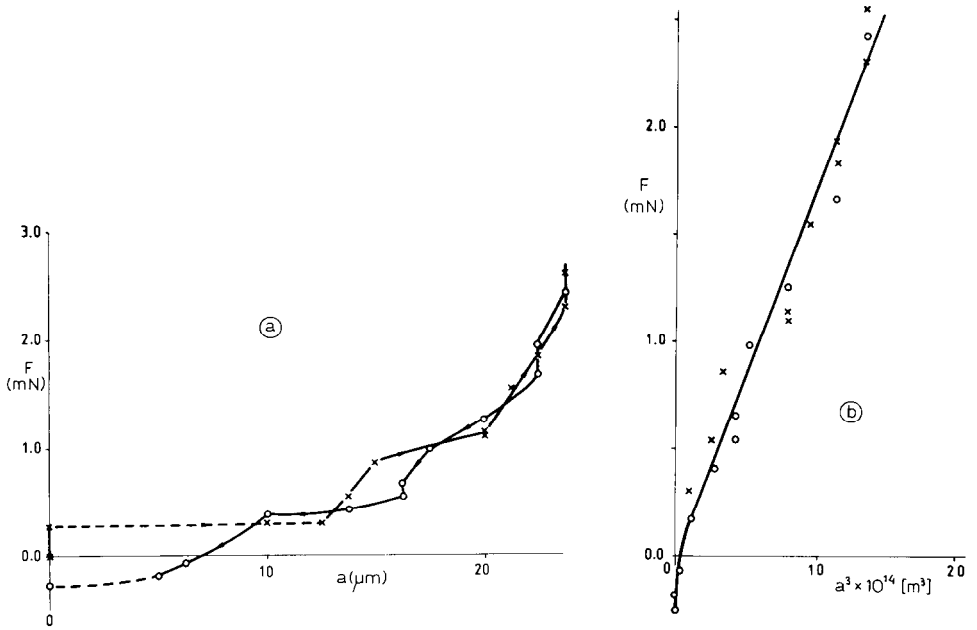

Fig. 1. The variation of the area of flat mica with the effective applied force F. EL/W, 50/50 (w/w) in liquid water, 24°C. a radius of contact area. (a) x, increasing F; ○, decreasing F. (b) Plot of F vs a^3, according to Eqn (1). The "contact" rupture occurred at −0.26 mN.

automatic micropipette between the widely separated (1—2 mm) mica surfaces and allowed to equilibrate (temperature, water content and distribution, etc.) overnight.

The force-measuring leaf spring supports the lower mica sheet [5]. Moving the leaf-spring clamp stepwise upwards (downwards), we modified accordingly the force on the sample which was subsequently squeezed out (sucked in). On the very first compression of a sample from an initial large separation of mica surfaces $D \simeq 1\ \mu m$, a significant force built up before the mica surfaces jumped to a separation D_{min}, where they flattened. The average normal pressure or stress on the LSLC film of thickness D_{min} was obtained from the values of the force F and of the "circular" flattened-mica areas as follows: $P = F/\pi a^2$.

The ordinary refractive index, n, was measured at the separation D_{min} and at several larger time-independent separations D. The movement of the leaf-spring clamp was then reversed (sucking in mode) and D, a and n were measured (Fig. 1). First, the radius a decreased at practically constant D (within our experimental accuracy). Then it vanished and a tension built up which, at a threshold value, pulled the mica surfaces apart, i.e., the "contact" ruptured. At this point the tension in the system had not yet relaxed. At constant clamp position the leaf spring and the separation D between the mica surfaces relaxed (Fig. 2). The log $(D_\infty - D)$ versus time plot in Fig. 2 was obtained assuming that $t_\infty = 280$ min and $D_{t=\infty} = 289$ nm. Considering the large size of the samples studied, we assumed that after their relaxation the residual force was practically D independent; operationally, this reference force was equal to zero.

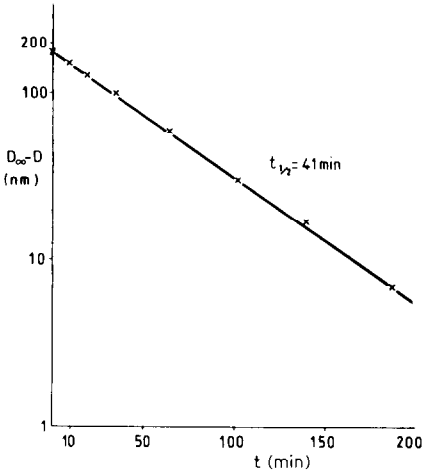

Fig. 2. Relaxation of surface separation as a function of time t to the equilibrium distance D_∞. Mixture II in the presence of liquid water at 24° C.

Refractive index

The optical method described in Ref. [5] was used to measure the variation of the average refractive index n of the LSLC thin films bounded by the mica surfaces at separations D. The error in n was largest at the smallest separation. It became $\Delta n = \pm 0.04$ for $D \simeq 10$ nm and $\Delta n = \pm 0.01$ for $40 < D < 150$ nm.

X-ray diffraction experiments [4] showed that EL molecules orientate normally to the plane of the layers. We assume (see Discussion) that the plane of the layers was parallel to the mica surfaces. Therefore, as the incident light was normal to them, it was parallel to the acyl chains of the EL molecules and the measured average refractive index n was the ordinary one, n_0.

RESULTS

Compression and decompression experiments

Figures 3, 4 and 5 reproduce the variation of the force F with separation D on compression. The values obtained for the refractive index n are shown in Fig. 6.

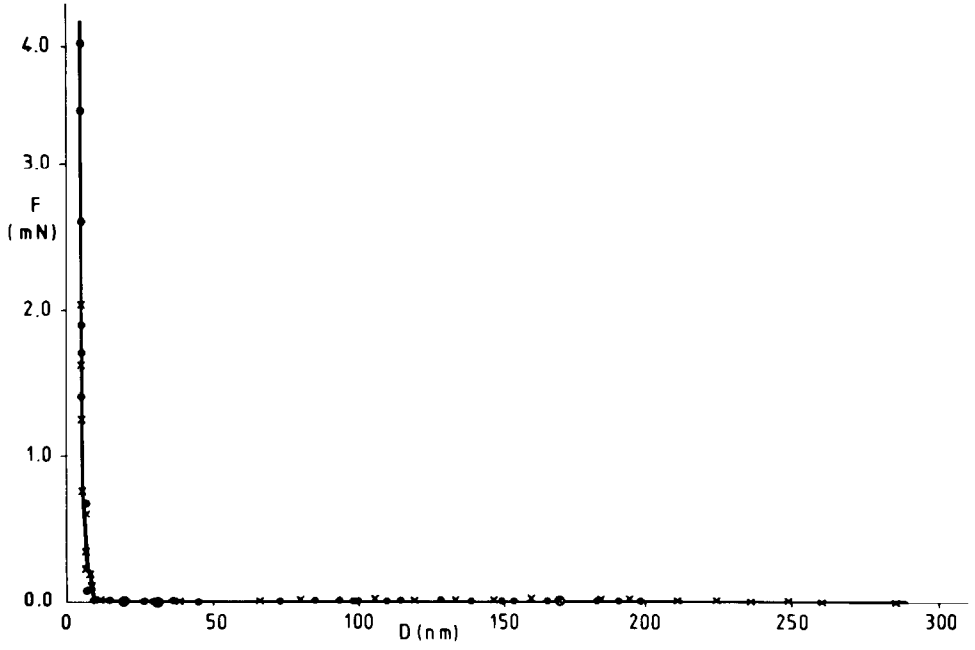

Fig. 3. Variation of the load F with the separation D between the mica surfaces for the EL/W mixture III. t = 20.5 ± 0.5°C. (x), In saturated water vapour; (•), in liquid water.

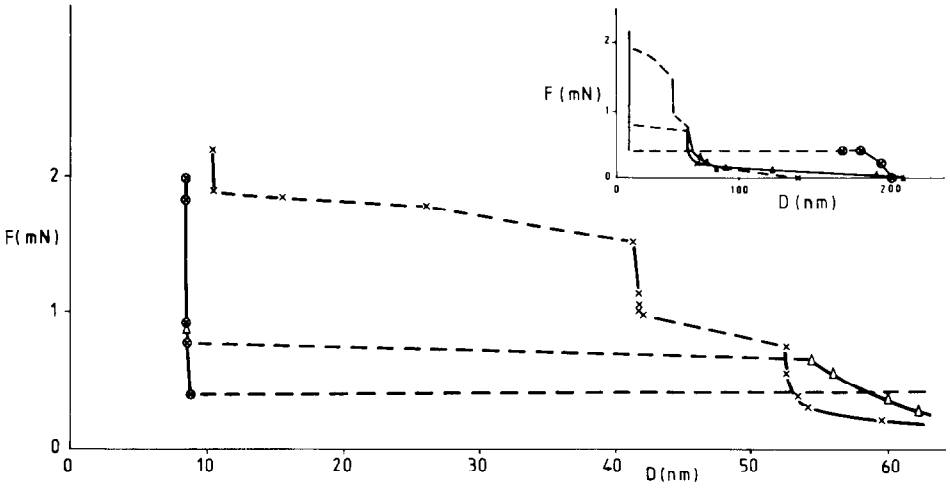

Fig. 4. Variation of the load F with the separation D between the mica surfaces for the EL/W mixture II, at t = 24 ± 1°C. × , In saturated water vapour; (x, △), in liquid water. Dashed line: D-instability or jump. Full line: gradual variation of D.

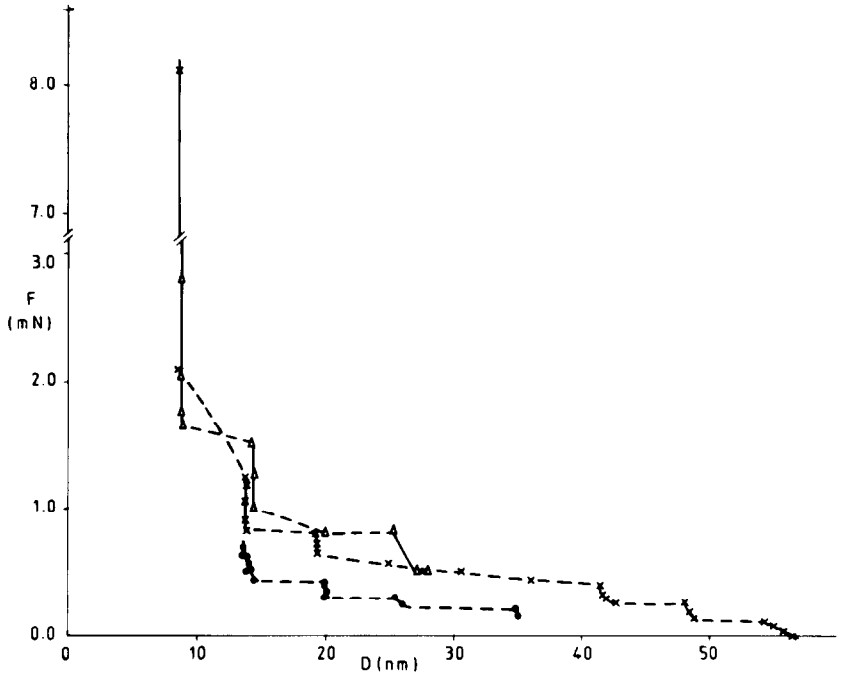

Fig. 5. Variation of the load F with the separation D between the mica surfaces for mixture I at t = 23.5 ± 1°C. In water-saturated vapour only.

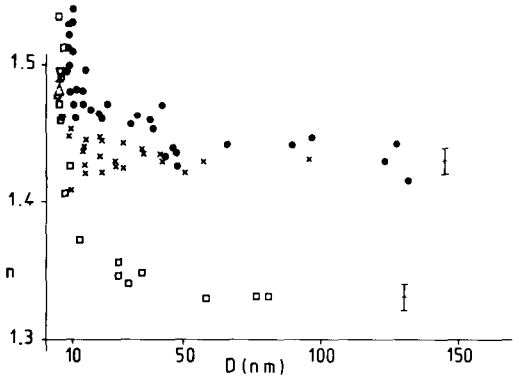

Fig. 6. Average ordinary refractive index n variation with the separation D. $20.5 < t < 24.5$°C. (x) Mixture I; (•), mixture II; (□), mixture III. (△) Quoted from Ref. [8]; (*), quoted from Refs. [6] and [7].

(a) 30/70 (w/w) EL/W samples (Fig. 3)

In the presence of both water vapour and liquid water at 20.5 ± 0.5°C this sample thinned down to $D < 10$ nm under negligible (< 0.05 mN) compressing forces. No major stepwise variations in the separation D were noticed. The mica sheets flattened at $D_{min} < 5.0 \pm 0.1$ nm. The values of the average normal pressure P obtained from the data are shown in Table 1. It is about 8×10^8 mN m^{-2}. Increasing P ten times reduced the separation D by 0.5 ± 0.1 nm.

(b) 50/50 (w/w) EL/W samples (Fig. 4)

In one experiment, carried out in the presence of saturated water vapour, the LSLC compression started at $D \simeq 200$ nm, then allowed the build-up of a significant force (0.42 mN), at which the sample yielded and thinned down to $D_{min} = 8.7 \pm 1$ nm where the mica sheets flattened. Increasing the stress to above 9.0×10^8 mN m^{-2}, the separation D_{min} shifted to 8.4 nm (Table 1). From the values of D_{min} and F, where the mica sheets flattened, the average value of $D_{min} = 9.4 \pm 1$ nm and $P = 3.5 \times 10^8$ mN m^{-2} were obtained from three runs.

For experiments carried out in the presence of liquid water, the runs are shown in Fig. 4. One was started at $D = 150$ nm. On applying a force of 20 μN the sample thinned down to 60 nm. On increasing the force F, compression instabilities occurred at $D = 52.5$ nm, $D = 41.3$ nm, $D = 26.0$ nm and $D = 15.5$ nm. The second run was started at $D = 210$ nm. This sample thinned gradually down to $D = 54$ nm at $F = 640$ μN. Then it yielded and thinned to $D_{min} = 8.4$ nm at $F = 780$ μN and $P = 2.7 \times 10^8$ mN m^{-2}. No stepwise thinning was observed, as for the experiment carried out in the presence of saturated water vapour. The major compression instability occurred, in liquid water and in vapour, at almost the same force F (see Fig. 4) but at different separations: at $D = 54.5$ nm in liquid water and at $D = 180$ nm in vapour.

TABLE 1

The variation of the separation D between the flattened-mica surfaces, with the load F and the normal stress P applied to thin films of EL/W mixtures

EL/W (w/w) (environment)	D[a] (nm)	F (μN)	P[a] $\times 10^{-8}$ (mN m^{-2})
60/40 (water vapour)	25.4	294	4.5
	19.9	419	4.4
	14.4	434	4.6
	14.0	472	5.0
	14.0	507	5.4
	13.6	760	7.0
	19.3	700	8.0
	13.8	1200	9.6
	8.8	2000	12.6
	8.8	2800	13.0
50/50 (vapour)	8.7	400	4.2
	8.5	930	4.7
	8.5	1840	9.0
	8.4	2000	N.D.[b]
50/50 (liquid water)	8.4	780	2.7
	10.4	1900	N.D.
	10.4	2200	N.D.
30/70 (water vapour and liquid water)	5.1	760	8.0
	5.0	1620	13.0
	5.0	2040	14.0
	4.4	3820	91.0

[a]Measured values (non-averaged).
[b]N.D. = not determined, i.e., the radius of the flat-mica surface was not measured.

Although the thinning pattern of the two samples of mixture II were not identical, the values of D_{min} and of the stress P were the same whatever the environment. In the presence of saturated vapour, values of D_{min} = 8.5 nm and $P = 4.4 \times 10^8$ mN m^{-2} $\pm$ 0.3×10^8 were found. We obtained values of D_{min} = 8.4 nm and P = 2.7 mN m^{-2} in the presence of liquid water (see Table 1). Therefore, the stepwise thinning process is not reproducible for mixture II. When stepwise thinning occurred, the steps ΔD were multiple of $\lambda = 5.3 \pm 0.3$ nm.

(c) 60/40 (w/w) EL/W samples (Fig. 5)

This sample was studied only in the presence of saturated water vapour at 23.5 $\pm$ 1.2°C. It was a thick paste. Compressed between mica surfaces, initially at a separation D = 700 nm, it yields at about F = 1 mN. This value is close to that observed for the 50/50 (w/w) EL/W sample studied in the presence of saturated water vapour (Fig. 4).

The results shown in Fig. 5 have been obtained with samples which

have been allowed to relax at smaller separations D (several tens of nanometers) between the mica surfaces. The thinning always proceeded stepwise. The steps in the three runs shown in Fig. 5 were equal to $\lambda = 5.5 \pm 0.4$ nm. In contrast to the mixtures discussed under (*a*) and (*b*), the mica sheets were flat at several separations larger than D_{min}, as shown in Table 1. For this sample, which is a homogeneous LSLC, the average value of a D-step is the same when the mica sheets are either flat or curved. Also, the smallest separation $D_{min} = 8.6$ nm is close to that displayed by the mixture 50/50 (w/w) EL/W.

The decompression of the samples did not show stepwise thinning, in general. On decreasing the force, the contact diameter decreased reversibly at constant D_{min} separation and no time effects were noticed under these conditions (Fig. 1). The scattering of the results shown in this Figure originated in the low accuracy of the values obtained for the radius a.

In general, at a given tension (negative force F) the mica surfaces drew apart from the separation D_{min} to a much larger D.

Refractive index

The values of the average refractive index n obtained for the EL/W mixtures I, II and III under the various conditions and separations D in the temperature range 20.5—24.5°C are shown in Fig. 6. For all the mixtures, n decreased with separation D. The decrease was larger for mixture III, which contained the largest amount of excess water, as if it were selectively squeezed out when the separation D decreased and the force F increased. For mixture III, the refractive index value $n = 1.33 \pm 0.01$, measured at large separations ($D \simeq 100$ nm) was very close to that of pure water ($n = 1.335$). Mixture II, which had less excess water, displays a similar D-dependence of n, but the value of the refractive index $n = 1.46 \pm 0.01$ at $D > 60$ nm is higher. Such a value has been obtained for the ordinary refractive index of black lipid membranes [6]. Finally, the homogeneous LSLC (mixture III) did not display any change of the refractive index with separation D. The average value obtained, $n = 1.43 \pm 0.05$, was smaller than that of mixture II. It is interesting to point out that at D_{min}, when the mica surfaces are flattened, the average water content of samples I, II and III did not significantly affect the value of the refractive index. The highest values measured for samples II and III at D_{min} cannot be explained, while the smallest ones are consistent with those reported in Refs. [6—8]. However, such unexpectedly high values for the refractive index, corresponding to solid paraffins, have been reported for liquid paraffins and hydrocarbons squeezed out between mica surfaces [9]. Finally, when the value of the refractive index n at large separation D was substracted from that measured at D_{min}, a shift Δn was obtained for the mixtures I, II, III studied. These shifts are equal to $\Delta n \simeq 0$, 0.2 ± 0.05 and 0.7 ± 0.05, respectively. They increase with the amount of excess water in the EL/W mixtures.

Elastic behaviour of the mica sheets and adhesion in the presence of EL/W mixtures

This behaviour was mainly studied using mixture III. Prior to the flattening of the mica sheets, the compression—dilation process was not reversible. The large hysteresis was probably due to the sample viscoelasticity. However, at the D_{min} separation, the deformation of the mica sheets, as estimated from measurement of the "contact" flat area radius a by the applied load F, was reversible (see Fig. 1a). A negative force F or tension was required to rupture the "mica—mica" contact. The average value obtained from three measurements for $(F/R)_{a=0}$ was 0.20 ± 0.10 mN.

To understand the origin of these results, we used the theory of Johnson et al. [10], which describes the deformation of two elastic adhering spheres at contact, applying it to our composite system formed by the curved-mica sheets and their polymeric-glue substrate. According to Ref. [10], the relation between the applied load F and the radius of the circular contact area is given by the following equation

$$(R/K)a^3 = F + 3\gamma\pi R + \{6\gamma\pi RF + (3\gamma\pi R)^2\}^{1/2} \quad (1)$$

where γ is the free energy of adhesion of the surfaces and K is a characteristic elastic parameter. In the case of the elastic-sphere model, which is a rough one for our composite mica-sheet—glue system, K is an effective elastic parameter. When $F \gg 3\gamma\pi R$, F becomes proportional to a^3 (Fig. 1b), according to Eqn (1). The results, too scattered, were not interpreted. The low accuracy of the measured values of the radius a resulted in large scattering of the values of a^3. The absence of time effects, when the mica sheets flattened, and the straight line shown in Fig. 1b at large forces F, allowed us to conclude that the viscoelastic effects were not involved under these conditions. Then, the average stress or normal pressure $P = (F/\pi a^2)$ was deduced (see Table 1). According to Eqn (1) the tension $-F = {}^3/_2\,\pi\gamma R$ at $a = 0$ is independent of the elastic behaviour of the deformable mica-sheet—glue system. The mica-sheet radius of curvature was equal to $R = 0.87 \times 10^{-2}$ m. The values of the free energy of adhesion γ of the mica sheets separated by a film of thickness $D_{min} = 9$ nm of the EL/W mixture II were in the range 2—6 mN m^{-1}. This value is of the same order of magnitude as that reported for rubber—rubber adhesion immersed in water, namely ~ 7 mN m^{-1} [12]. We do not speculate on our values of γ at present.

DISCUSSION OF THE RESULTS

Our experiments were carried out in the temperature range 20.5—24.5°C. However, the structure of EL—LSLC displays no discontinuity in this range [4].

Whatever its origin and nature, the force F and the related pressure

affect the hydration of EL bilayers and the LSLC repeat distance, which varies with any applied pressure [3]. Then, if a compression instability sets in, e.g., by defect formation and bilayer rupturing, the stepwise thinning which occurred in samples I and II should be related to the value of the repeat distance λ at the average normal pressure or stress set up on the thin liquid film of LSCL, of thickness D, limited by the mica surfaces before it flattened. The stepwise-thinning behaviour of mixtures I and II gives us information on the orientation of the LSLC on mica: the planes of the bilayers are parallel to the mica surfaces. For sample I, the homogeneous LSLC (60/40 (w/w) EL/W), the values of λ are equal to 5.5 ± 0.4 (Fig. 5) and the compression instabilities occurred at stresses in the range 4.5—13 mN m^{-2}. At such applied pressures, the repeat distance [3] varies in the range $\lambda = 5.4 \pm 0.3$ nm for the bulk EL—LSLC. The agreement between our results and those of Ref. [3] may only be a coincidence. We noticed that sample III (30/70 (w/w) EL/W), which did not display stepwise thinning, was not viscoelastic. The variation of its refractive index with separation D was largest (Fig. 5) while at D_{min} this index was independent of the water concentration in the sample. This may be explained by the very heterogeneous structure of this mixture, probably consisting of a dispersion of large liposomes in water which are trapped between the mica surfaces. When compressed, the excess water is selectively extruded from the trapped liposome dispersion.

Mixture II (50/50 (w/w) EL/W) has a composition which is intermediate between that of mixtures I and III, thus it displays the thinning patterns of both these mixtures. When it thinned stepwise (Fig. 4), the steps ΔD were multiples of $\lambda = 5.3 \pm 0.3$ nm. Finally, the variation of the mixture II refractive index with separation D was intermediate between that of samples I and III.

The minimum separation D_{min} is determined by the mixture composition and the deformability of the mica sheets. At the maximum stress available (see Table 1), the average value $D_{min} = 9 \pm 0.7$ nm was obtained for the three samples of mixtures II and two samples of mixture I. This value of D_{min} is smaller than that of twice the average value of $\lambda = 5.4 \pm 0.4$ nm corresponding to samples I and II.

We speculate that these flat, thin LSCL films consist of either one overhydrated bilayer (Fig. 7a) or two bilayers, mostly dehydrated at their contacts with the mica surfaces (Fig. 7b). Possibly, the large dipoles of the outer EL molecules orientate their large dipoles parallel to the tangential electrostatic field of the mica surfaces, as described by Muller and Chang [11]. This interaction may enhance the order of the acyl chains belonging to the EL molecules which are nearest to mica and decay with distance from the mica surfaces.

Using the results reported in Ref. [3], namely $\lambda = 5.4$ nm, $d_w = 1.6$ nm and $d_e = 3.8$ nm (where d_e is the lipid bilayer thickness) corresponding to an applied pressure of 10 mN m^{-2}, we estimate the lipid volume fractions ϕ corresponding to the models shown in Figs. 7a and 7b for the separation D_{min}, assuming that $d_e = 3.8$ nm for both models. We obtain ϕ

(Fig. 7a) = 0.43 and ϕ (Fig. 7b) = 0.84, respectively. The large average values of the refractive index displayed by the thin films of LSLC at D_{min} (Fig. 6) point in favour of the model shown in Fig. 7b.

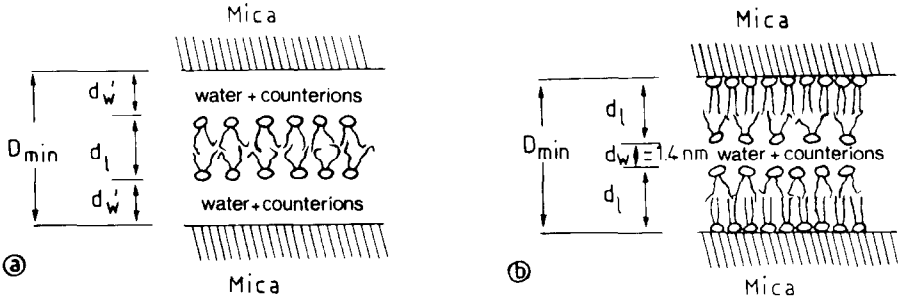

Fig. 7. Structure of the EL/W—LSLC thin film at D_{min} = 9.0 ± 0.7 nm. (a) d_l = 3.8 nm; d_w = 2.6 nm. (b) d_l = 3.8 nm; d_w = 1.4 nm.

For the dilute mixture III (30/70 (w/w) EL/W) the value of D_{min} = 4.4 nm has been obtained at a very large stress. It corresponds to one bilayer of EL and to a hydration of one monolayer of water molecules on each side. The lipid mole fraction at this value of D_{min} is ϕ = 0.86. The high value of the refractive index, n = 1.5, verifies this model for the more dilute EL/W mixture III.

The low and D-independent value of the refractive index of sample I n = 1.43 might be due to the high viscosity of this sample, which did not allow selective extrusion of the water from the mica—bilayer interface.

CONCLUSION

The compression of concentrated dispersions of EL in water between mica surfaces involves the entrapment of lipid multibilayers or liposomes between the solid surfaces and selective extrusion of the excess water phase, as well as of most of the water molecules at the bilayers—mica interface. At large stresses, when the mica sheets flattened, the lipid bilayers, oriented parallel to the mica surfaces, form a thin LSLC film of EL. At mica separations of the order of about ten parallel bilayers, a stepwise-thinning process is observed for the most concentrated dispersions of EL. The steps are related to the repeat distance of the LSLC at the pressure supported by the thin film of EL.

ACKNOWLEDGEMENTS

The authors acknowledge particularly interesting discussions with E. Evans, R. Horn, J. Israelachvili, J. Klein, V.A. Parsegian, A. Roberts, E. Sackmann, A. Silberberg and D. Tabor. Mrs Albrecht and G. Madelmont prepared the studied samples.

REFERENCES

1 R.G. Horn, J.N. Israelachvili and E. Perez, J. Phys., 42 (1981) 39.
2 L. Ter-Minassian-Saraga and E. Perez, Journées Colloides et Interfaces, Collège de France, Paris, 29—30 November, 1982.
3 D.M. Le Neveu, R.P. Rand, V.A. Parsegian and D. Gingell, Biophys. J., 18 (1977) 209.
4 F. Reiss-Husson, J. Mol. Biol., 25 (1967) 363.
5 J.N. Israelachvili and G.E. Adams, J. Chem. Soc. Faraday Trans. 1, 74 (1978) 975.
6 R.J. Cherry and D. Chapman, J. Mol. Biol., 40 (1969) 19.
7 R.J. Cherry and D. Chapman, J. Mol. Biol., 30 (1967) 551.
8 C. Huang and T.E. Thompson, J. Mol. Biol., 13 (1965) 183.
9 L.R. Fisher and J.N. Israelachvili, J. Colloid Interface Sci., 80 (1981) 528.
10 K.L. Johnson, K. Kendall and A.D. Roberts, Proc. R. Soc. London, Ser. A, 324 (1971) 301.
11 K. Muller and C.C. Chang, Surface Sci., 14 (1969) 39.
12 A.D. Roberts and D. Tabor, Proc. R. Soc. London, Ser. A, 325 (1971) 323.